Physiological differences among cryptic species of the Mediterranean crustose coralline alga Lithophyllum stictiforme (Corallinales, Rhodophyta)

Sophie Martin, Virgile Calvert, Anne Chenuil

PHYSIOLOGICAL DIFFERENCES AMONG CRYPTIC SPECIES OF THE MEDITERRANEAN CRUSTOSE CORALLINE ALGA *LITHOPHYLLUM STICTAEFORME*/*CABIOCHAE* (CORALLINALES, RHODOPHYTA)

Sophie MARTIN*

CNRS, Sorbonne Université,

UMR 7144, AD2M, Adaptation et Diversité en Milieu Marin, Station Biologique de Roscoff,

Place Georges Teissier, 29680 Roscoff, France

E-mail address: sophie.martin@sb-roscoff.fr, Phone / Fax: +33 (0)2 98 29 56 59 / 23 24

Virgile CALVERT

Aix Marseille Univ, Avignon Univ, CNRS, IRD,

IMBE, Institut Méditerranéen de Biodiversité et d'Ecologie, Station Marine d'Endoume,

Chemin de la Batterie des Lions, 13007 Marseille, France

Anne CHENUIL

Aix Marseille Univ, Avignon Univ, CNRS, IRD,

IMBE, Institut Méditerranéen de Biodiversité et d'Ecologie, Station Marine d'Endoume,

Chemin de la Batterie des Lions, 13007 Marseille, France

Short running title: **CCA cryptic species physiology**

* Corresponding author: smartin@sb-roscoff.fr

ORCID: https://orcid.org/0000-0002-1256-3674

ABSTRACT

The crustose coralline alga *Lithophyllum stictiforme/cabiochiae* is an important bioconstructor of coralligenous concretions in the Mediterranean Sea. This algal species complex is composed of several cryptic species. Here, we compared light-dependent physiological processes within and between cryptic species of *L. stictiforme/cabiochiae* from the Bay of Marseille (France). We measured summer rates of respiration, photosynthesis, and calcification by using incubation chambers under various irradiance levels and in the dark. We compared the physiology of the cryptic species C1, the most common of the complex, and C4 from the same locality (shallower site at 28-m depth) and C1 from a deeper site at 45-m depth. We pointed out both interspecific (between C1 and C4) and intraspecific (within C1) physiological differences. Photosynthetic parameters showed acclimation to light (or depth) with lower values of saturating irradiance E_k and compensating irradiance E_c for C1 from 45-m than those from 28-m depth. Within the shallower site, significant physiological differences were observed between C1 and C4 with higher rates of gross photosynthesis $P_{g\,max}$ and diel 24-h net production in C4, suggesting better ability to grow under high irradiance. Light and dark calcification rates differed only between C4 from 28-m and C1 from 45-m depth, while they were intermediate in C1 from 28-m depth. On a 24-h basis, diel net calcification rates were significantly higher in shallower specimens than in deeper ones. Physiological differences suggest both physiological plasticity within the dominant and ubiquitous cryptic species C1 and species-specific physiological traits between the cryptic species C1 and C4.

HIGHLIGHTS

- Photosynthesis and calcification rates differ among *Lithophyllum stictiforme/cabiochiae* cryptic species
- The dominant and ubiquitous cryptic species exhibits light-dependent physiological plasticity
- Physiological differences exist between cryptic species found in similar environment

KEYWORDS: Calcification, coralline algae, cryptic species, depth, *Lithophyllum*, photosynthesis, physiology, light

INTRODUCTION

Crustose (nongeniculate) coralline algae (CCA) are marine red algae (Rhodophyta) of the family Corallinaceae. They are characterized by a calcareous thallus because of extensive crystalline calcium carbonate deposits within the walls of their vegetative cells. CCA occur worldwide from polar regions to the tropics (Johansen, 1981; Steneck, 1986) and occupy the entire depth range inhabited by photosynthetic organisms, from the surface to depths below 200 meters (Littler *et al*., 1991); some under intense illumination, others in very dim light conditions. They are key ecosystem engineers that produce or consolidate biogenic benthic habitats. In the Mediterranean Sea, CCA are the main builders of a typical habitat named coralligenous. The coralligenous represents the unique calcareous formation of biogenic origin in the Mediterranean Sea (Ballesteros, 2006) and is considered as the second Mediterranean benthic key-ecosystem in terms of biodiversity, after *Posidonia oceanica* meadows. The complex structure of the calcareous coralligenous concretions allows the development of a high species diversity belonging to taxonomic groups as diverse as algae, sponges, gorgonian corals, molluscs, echinoderms, bryozoans, polychaetes, tunicates, crustaceans or fishes, which live over the concretions (epiflora and epifauna), in the small holes and crevices of the coralligenous structure (cryptofauna), inside the concretions (borers), and even in the sediment deposited in cavities and holes (endofauna ; Ballesteros 2006). This habitat provides a diversity of ecosystem services including original resources for local fisheries and beautiful seascapes for recreational scuba-diving (Thierry de Ville d'Avray *et al*., 2019).

Mediterranean coralligenous concretions thrive exclusively in dim light conditions, mainly in deep waters (20-120 m depth) where irradiance is reduced to between 0.05 and 3% of the surface irradiance (Ballesteros, 2006). In these environments of low-light conditions, the main coralligenous-forming CCA are species of genus *Lithophyllum*, previously described as *L. stictiforme* (Areschoug) Hauck (1877) and *L. cabiochiae* (Boudouresque & Verlaque) Athanasiadis (1999) (Sartoretto *et al*., 1996). These common CCA species are known to play a major role on the development and biodiversity of coralligenous assemblages. *L. stictiforme* has been shown to favor establishment of other species of the coralligenous reefs, through algal and invertebrate recruitment on their thalli (Piazzi *et al*., 2022).

The *L. stictiforme/cabiochiae* species complex is the single important bioconstructor which is widespread across the whole Mediterranean basin. This nominal species however does not correspond to a single evolutionary unit since it is composed of several biological species which are reproductively isolated, named cryptic species (De Jode *et al*., 2019;

Pezzolesi *et al*., 2019). Ignoring cryptic species, which are frequent in marine species, may cause overestimation of the distribution range size (or niche width), when distinct cryptic species have differentiated distributions (or niches, respectively) (Chenuil *et al*., 2019). Such errors, particularly when affecting keystone species, may have serious consequences in ecosystem monitoring/management. In *L. stictiforme/cabiochiae*, eight cryptic species (C1 to C8) are found in sympatry in the Bay of Marseille (Northwestern Mediterranean Sea; De Jode *et al*., 2019). Spatial distributions of these cryptic species are overlapping but their relative abundances are significantly differentiated according to depth and irradiance, suggesting their niches are differentiated (De Jode *et al*., 2019). Irradiance is effectively the most important environmental factor shaping coralligenous communities (Ballesteros, 2006). The distribution of the cryptic CCA engineering species according to irradiance potentially has important consequences on the composition of these communities (De Jode *et al*., 2019). Although the cryptic species of the *L. stictiforme/cabiochiae* complex are adapted to low values of irradiance, their light-dependent ecological and physiological traits are likely to vary among cryptic species.

Before cryptic species were evidenced, Martin *et al*. (2013a,b) had studied physiological responses to irradiance of *L. cabiochae* collected in the Bay of Villefranche (NW Mediterranean) at 25-m depth. They have shown that both photosynthesis and calcification were strongly dependent on irradiance in this species. Although poorly documented, physiological differentiation has already been observed among cryptic marine red macroalgal species of the families Delesseriaceae and Rhodomelaceae (Kamiya *et al*., 2014; Muanmai *et al*., 2015). If this physiological differentiation occurs to adapt to particular environments, then cryptic species may perform in different ways in response to specific environmental factors. As previously reported for other temperate coralline algae (Martin *et al*., 2006; Martin & Hall-Spencer, 2017), respiration, photosynthesis, and calcification processes in *L. cabiochae* are strongly influenced by the seasonal variations of both irradiance and temperature and are the highest in summer when temperature and irradiance levels are maximal (Martin *et al*., 2013b). In addition to their metabolism, both survival and reproduction have also been reported to depend on temperature and irradiance in *L. stictaeforme* collected at 30-35 m depth in the NW Mediterranean (Rodríguez-Prieto, 2016). In these studies, species were identified ignoring the presence of cryptic species and thus missing potential differences of responses of cryptic species to these environmental factors.

In the present study, we measured physiological rates of *L. stictaeforme/cabiochae* in the summer period, likely under optimal conditions of temperature and irradiance. In their

natural environment (from 28 to 45-m depth) along Marseille's coastline, *L. stictaeforme/cabiochae* cryptic species are exposed to comparable temperature values since they grow below the summer thermocline threshold (Harmelin, 2004; Haguenauer *et al*., 2013). Therefore, De Jode *et al*. (2019) considered irradiance as the main environmental factor of differentiation between cryptic species. Here, we compared light-dependent physiological processes (i.e. photosynthesis and calcification) of two of the cryptic species of the complex *L. stictiforme/cabiochiae*, one, clade C1, which is the most abundant around Marseille coastline and present at all depths (from shallowest to deepest sites) and, the other, clade C4, which is less abundant and mainly found in the Northern sector of the Bay of Marseille at shallowest depth (De Jode *et al*., 2019). Photosynthetic and calcification processes being dependent on the availability of light (Martin *et al*., 2013a,b), we assessed the physiological performances of *L. stictiforme/cabiochiae* cryptic species through measurements of their specific photosynthetic parameters derived from photosynthesis-irradiance curves and of their specific photosynthetic and calcification rates under in situ representative irradiances. Photosynthetic and calcification responses under various irradiance levels allowed us (i) to identify potential physiological differences between the cryptic species and/or localities (depths) and (ii) to see if the cryptic species with a larger distribution (C1 species) has greater physiological abilities. Two sites at two distinct depths were chosen to allow interspecific comparisons at similar depths and intraspecific comparisons at different depths.

MATERIALS AND METHODS

Study site and biological material

Specimens of the species complex of crustose coralline algae *Lithophyllum stictaeforme*/*cabiochae* were collected in coralligenous habitats of the Bay of Marseille (France), a semi-opened embayment (about 40 km by 25 km, from the Gulf of Fos to the Riou archipelago) located in the Northwestern Mediterranean Sea. Two cryptic species (or clades, C1 and C4) were chosen, based on their field distributions (De Jode *et al*., 2019), so that they have differential environmental preferences, are found in the same environment in at least one locality (in syntopy), and are relatively abundant to obtain sufficient individuals of each species for our experiment. Individuals were sampled by scuba divers in two localities at distinct depths, based on previous knowledge on the relative abundances of C1 and C4 cryptic species (De Jode *et al*., 2019): (i) "La Couronne" (LC) in the Northern sector of the Bay of Marseille at *ca*. 28-m depth (43°19.668'N, 5°1.775'E) on 9 July 2018 and (ii) "Riou-Moyade" (RM) in the Riou archipelago in the Southern sector of the Bay of Marseille at *ca*. 45-m depth (43°10.574'N, 5°22.208'E) on 11 July 2018 (Fig. 1). According to De Jode *et al*. (2019), two cryptic species (C1 and C4) have been found at LC, while only one cryptic species (C1) was found in deep waters (37-46-m depth) at RM. Light and depth were homogeneous for all collected specimens at each sampling site, even at LC, where C1 and C4 co-occur in similar light conditions. The slope of the substrate was similarly inclined at LC and RM, while light exposition of the substrate was South-West at LC and East at RM (De Jode, 2018).

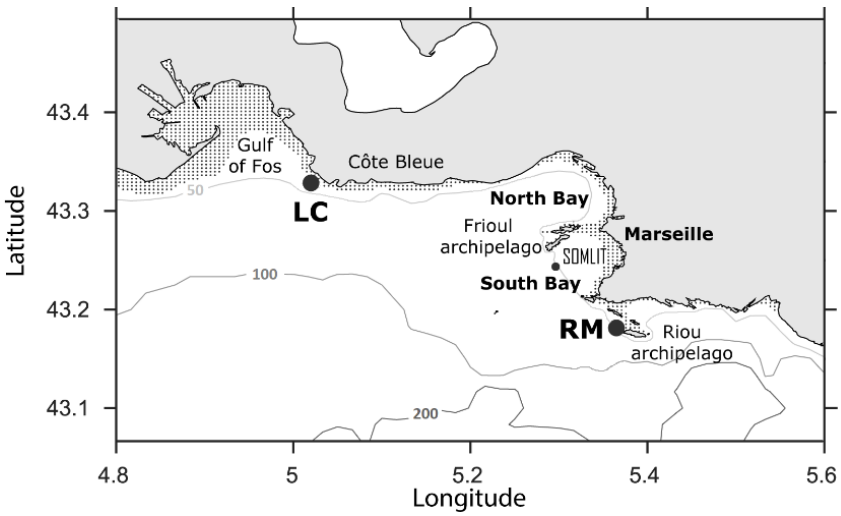

Fig. 1. Map of the study area, showing the locations of the two sampling localities in the Bay of Marseille: La Couronne (LC) and Riou-Moyade (RM). SOMLIT: Frioul station

(*ca*. 65-m depth) of the French national network of coastal observation CNRS-INSU SOMLIT (*Service d'Observation en Milieu Littoral*).

Photosynthetically available radiation (PAR; µmol photons m^{-2} s^{-1}) at 28 and 45 m depth in the Marseille Bay was calculated from surface PAR and vertical PAR attenuation coefficient (K_{PAR}) for a typical month of July. K_{PAR} was calculated according to Kirk (1994) from vertical irradiance profiles obtained in the Bay of Marseille at the SOMLIT Frioul Station on 4 separate dates (July 11 and 25, 2018, and July, 11 and 23, 2019). The mean K_{PAR} were 0.094 and 0.085 m^{-1} at 28 m and 45 m depth, respectively. They were used in combination with the incident PAR at the surface to determine the daily cycle of irradiance at 28 and 45 m depth (Fig. 2). The incident PAR at the surface was measured on July 2007 using a flat quantum sensor (LI-COR, LI-192SA) at Saint-Jean- Cap-Ferrat located at similar latitude (43,7°), 150 km east of Marseille on the French Mediterranean coastal areas. In the Bay of Marseille in July, the mean maximal PAR at noon was 135 µmol photons m^{-2} s^{-1} at 28 m depth and 40 µmol photons m^{-2} s^{-1} at 45 m depth and the mean daily values were 70 and 20 µmol photons m^{-2} s^{-1}, respectively (Fig. 2).

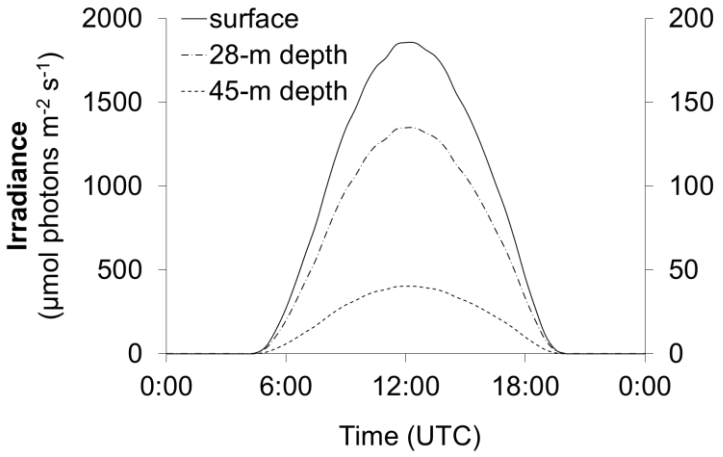

Fig. 2. Daily mean changes in incident photosynthetically available radiation (PAR) at the surface (left axis) and at 28 and 45 m depth (right axis) in July in the Bay of Marseille.

Algae were transported to the *Mediterranean Institute of Biodiversity and Ecology* (IMBE) in seawater in a thermostated tank to maintain samples at *in situ* temperature (ca. 16°C). Algae were thoroughly cleaned of epiphytic organisms without causing any damage to

the thalli. LC samples were divided in two groups of algae according to their morphology. The first group of algae from LC was characterized by a thinner and slightly more purple and rough thallus. It was identified as the clade C4 using further genetic analysis (see below). The second group of algae from LC was characterized by thicker and slightly pinker and smoother thallus; it was then identified as the clade C1 (Fig. 3). RM samples were all morphologically similar and characterized by a pink, smooth and thin thallus. Their identification as the clade C1 at this location by De Jode *et al*. (2019) was confirmed by genetic analysis. Differences in thickness, measured as surface to volume (S/V) and surface to weight (S/W) ratios were significant among algal groups ($p \leq 0.002$, Table 1, Figure S1). Both ratios were the lowest in the clade C1 from LC (28-m depth) and significantly (+50%) higher in the clade C1 from RM (45-m depth). The S/V and S/W ratios of clade C4 (LC) were intermediate and did not differ significantly from C1 from LC and RM.

From each of the three groups of algae (LC-C4, LC-C1, and RM-C1), 12 specimens with a flat thallus of *ca.* 20 cm^2 were selected for the experiments. At the end of the experiments, the algal volume was measured by displacement of water, considering that the algal volume submerged equals the volume of seawater displaced. It was determined on a balance to the nearest 0.01 g and converted to ml using the density of seawater. The algal fresh weight was determined to the nearest of 0.01 g after drying with a sorbent paper to remove seawater. The algal surface area was determined from photographs using the software Image J Version 1.8.0.

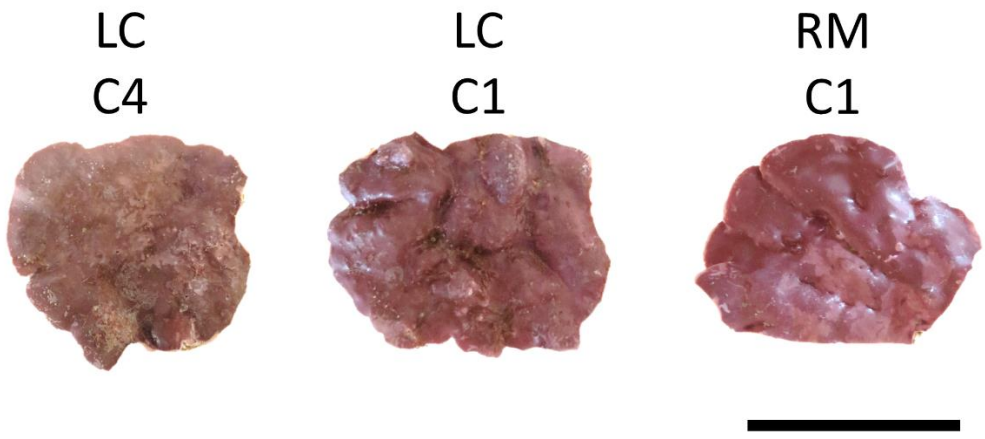

Fig. 3. Morphology of the *Lithophyllum stictaeforme*/*cabiochae* cryptic species C1 and C4 from "La Couronne" (LC) and "Riou-Moyade" (RM) localities. Scale = 5 cm. (Photo © S. Martin).

Genetic analyses

In order to identify the cryptic species for each sample, a piece of thallus was cut from each individual and frozen at -20°C until DNA extraction immediately after physiological experiments were achieved. DNA extraction, PCR (of a portion of the 28S ribosomal DNA) and Sanger sequencing were performed according to De Jode *et al*. (2019).

Experimental setup

Algae were maintained in aquaria continuously supplied with natural Mediterranean seawater pumped at 5 m depth in the Bay of Marseille in order to prevent any change in seawater composition. Temperature in the aquaria was adjusted to 16.0°C and controlled in the aquaria to within ± 0.1°C using a temperature controller (Model Teco TK 150). Salinity was measured with a conductivity probe (Horiba U-5000) and remained constant (37.9) during the experiment. The pH on the total scale (pH_T) was measured using a pH-meter (Mettler Toledo) calibrated on the total scale using Tris/HCl and 2-aminopyridine/HCl buffer solutions (Dickson et al. 2007). The $pH_{T\text{-}16°C}$ averaged 8,11 ± 0.02 (n = 8). For measurements of total alkalinity (A_T), seawater samples were filtered through 0.7 µm Whatman GF/F filters, immediately poisoned with mercuric chloride and stored in a cool dark place pending analyses. A_T was determined potentiometrically on 20-ml sub-samples using an automatic titrator (Titroline alpha, Schott SI Analytics, Germany) calibrated on the National Bureau of Standards scale. A_T was calculated using a Gran function applied to pH values ranging from 3.5 to 3.0 (Dickson et al. 2007) and corrected by comparison with standard reference material provided by Andrew G. Dickson (CRM Batch 111). Temperature, salinity, and parameters of the seawater carbonate system ($pH_{T\text{-}25°C}$ = 7.98 ± 0.02 and A_T = 2560 ± 2 µEq kg^{-1}, n = 8) in the aquaria were in the range of those measured at the SOMLIT (*Service d'Observation en Milieu Littoral*) Frioul Station in the Bay of Marseille (Fig. 1) on 11 July 2018, at 32-m depth (T = 16.6°C, S = 38.1, $pH_{T\text{-}25°C}$ = 7.97, and A_T = 2559 µEq kg^{-1}) and 55-m depth (T = 14.7°C, S = 38.2, $pH_{T\text{-}25°C}$ = 7.94, and A_T = 2562 µEq kg^{-1}) (Wimart-Rousseau et al. 2020). They were representative of those measured in July from 2016 to 2018 at these depths at the SOMLIT / Frioul Station (T = 15.6 ± 0.4°C, S = 38.2 ± 0.01, $pH_{T\text{-}25°C}$ = 7.95 ± 0.01, and A_T = 2584 ± 8 µEq kg^{-1}, n = 12).

The irradiance in the aquaria was set to mimic average daylight irradiance values in deep waters (30-45 m depth) of the Bay of Marseille in July. It was adjusted to *ca*. 20 µmol photons m^{-2} s^{-1} with an Apogee SQ-120 quantum sensor under controlled photoperiod of 12 h. The light was provided by a combination of Blue (450 nm) and Cool White (6500 K) LEDs (Alpheus Radiometrix EVO) above the aquaria.

Physiological measurements

Physiological measurements were performed after a one-day acclimation period under laboratory conditions. Algal physiology (photosynthesis, respiration and calcification) was assessed through two independent sets of light and dark incubation measurements. Physiological rates were measured in 100 or 185 mL transparent acrylic respirometry chambers (Engineering & Design Plastics Ltd, Cambridge, UK) filled with filtered seawater and continuously stirred with a magnetic stirring bar. The chambers were placed in a thermostated bath at 16.0°C, above which was installed similar light sources (Blue and Cool White LEDs) as above the aquaria. The intensity of photosynthetically active radiation (PAR) was adjusted using an Apogee SQ-120 quantum sensor and a computer-controlled system (Alpheus Radiometrix EVO).

Control incubations without algae were performed to check for biological activity in seawater. No significant activity (no difference from 0; t-test, $p > 0,05$) was detected in the seawater, whatever the irradiance levels.

Two sets of complementary measurements were performed in each group of algae: (i) a first set of incubations to determine photosynthetic parameters derived from the response curves of photosynthesis to irradiance (P-E) under a range of irradiance levels from 0 to 200 µmol photons m^{-2} s^{-1} and (ii) a second set of incubations to determine respiration, photosynthetic and calcification rates in the dark and under representative in situ irradiance at ca. 30-m and 45-m depth (ie 100 and 50 µmol photons m^{-2} s^{-1}, respectively).

(i) Photosynthetic parameters

The 12 selected specimens of each group of algae (LC-C4, LC-C1, and RM-C1) were incubated individually through independent dark and light incubations in 185 and 100 mL chambers, respectively. Respiration rates (R_d) were measured in the dark for 30 minutes after 1-hour exposure to the dark. Net primary production rates (P_n) were measured for 10 minutes

at each irradiance intensity given by the controlled LED-based light source in increasing orders (5, 10, 25, 50, 100, 150, and 200 µmol photons m^{-2} s^{-1}). Oxygen concentrations were measured at the beginning and at the end of each irradiance level using a non-invasive optical fiber system (FIBOX 3, PreSens, Regensburg, Germany). Reactive oxygen spots in the chambers were calibrated with 0% and 100% oxygen buffers.

As recommended by Martin & Gattuso (2009) and Martin *et al*. (2013a,b) for this species, physiological rates were normalized to thallus surface area since photosynthetic tissues are present in the living upper thallus layer of the crusts. Indeed, CCA metabolic rates are usually expressed per unit of crust surface to avoid any artefact due to the thickness of skeletal carbonate below the living coralline layer (Chisholm, 2003). This enables comparison of the physiological rates between algal groups of different surface to volume (or weight) ratios.

The rates of net photosynthesis (P_n) and dark respiration (consumption of O_2, R_d) (in µmol O_2 cm^{-2} h^{-1}) thallus were calculated following Eq. (1):

$$P_n \text{ (or } -R_d) = (\Delta O_2 \times V) / (\Delta t \times S) \quad (1)$$

where ΔO_2 is the difference between the initial and final oxygen concentrations (µmol O_2 L^{-1}), V is the volume of seawater in the chamber (the volume of the chamber minus the volume of the alga, L), Δt the incubation time (h), and S is the thallus planar surface area (cm^2).

Gross production (P_g) was calculated as the sum of $|P_n|$ and $|R_d|$.

The response of the photosynthetic oxygen-evolving rate to irradiance (E, µmol photons m^{-2} s^{-1}) was fitted with the model of Platt *et al*. (1980). Photosynthesis versus irradiance (P_n-E) curve parameters were obtained for each specimen according to Eq. (2):

$$P_n = P_{g\,max} \times (1 - e^{-\frac{E}{Ek}}) - R_d \quad (2)$$

where $P_{g\,max}$ is the maximum rate of gross photosynthesis (µmol O_2 cm^{-2} thallus h^{-1}), E_k (µmol photons m^{-2} s^{-1}) is the saturating irradiance (irradiance at which the initial slope intercepts the horizontal asymptote, µmol photons m^{-2} s^{-1}).

The compensation irradiance (E_c, µmol photons m^{-2} s^{-1}) is the irradiance at which P_n = 0 (or $P_g = R_d$).

(ii) Physiological rates of respiration, photosynthesis, and calcification

The first 6 of the 12 specimens of each group of algae (LC-C4, LC-C1, and RM-C1) were incubated individually through independent dark or light incubations in 100 or 185 mL chambers.

Dark respiration (R_d) and calcification (G_d) rates were measured in the dark for 2 hours in 185 mL chambers after 1-hour exposure to the dark. Net primary production rates (P_n) and light calcification (G) were measured for 1 h (in 100 mL chambers) or 2 h (in 185 mL chambers) at two irradiance levels of 50 and 100 µmol photons m^{-2} s^{-1}. The rates of R_d and P_n were determined from measurements of oxygen concentrations at the beginning and at the end of each incubation as described above. Net calcification rates in the dark (G_d) and light G) were estimated using the alkalinity anomaly technique (Smith & Key, 1975), which is a good estimator for short-term incubations. It is based on a decrease of 2 moles total alkalinity (A_T) by two equivalents per molecule of $CaCO_3$ precipitated (Wolf-Gladrow *et al*., 2007). Seawater was sampled at the beginning and at the end of incubation, and A_T analyses were performed as previously described.

Net calcification rates (G or G_d) were calculated as Eq. (3):

$$G \text{ (or } G_d) = (\Delta A_T \times V) / (2 \times \Delta t \times S) \quad (3)$$

where ΔA_T is the difference between initial and final A_T (µEq L^{-1}), V is the volume of the chamber (L), Δt is the incubation time (h), and S is the thallus surface of the algae (cm^2).

Diel carbon and carbonate production

Diel (24 h) P_n (or G) was calculated by summing daily P_n (or G) during the daylight period and R_d (or G_d) during the night-time period. Daily P_n was calculated by integrating the P_n (P_g or G) versus E curves against the incident irradiance at 28-m (LC) or 45-m (RM) depth in July in the Bay of Marseille during the daylight period (Fig. 1). The rates of P_n and R_d in µmol O_2 cm^{-2} h^{-1} were converted to µmol C cm^{-2} h^{-1} using the photosynthetic (PQ = $P_{n\,O2}$ / $P_{n\,CO2}$ = 1) and respiratory (RQ = $R_{d\,CO2}$ / $R_{d\,O2}$ = 1) quotients previously reported for *Lithophyllum cabiochae* (Martin *et al*., 2013a). Daily G was estimated from linear relationship between 0 and mean maximal *in situ* incident irradiance (ie. 100 µmol photons m^{-}

^{2} s^{-1} at LC and 50 µmol photons m^{-2} s^{-1} at RM) since the rate of calcification increases linearly with the light intensity while the rate of calcification saturates around maximal *in situ* irradiance level (Martin *et al*., 2013a,b).

Statistical analyses

Results are expressed as mean ± standard error of the mean (SE).

Differences in morphological and physiological parameters between algal groups were tested by using one-way ANOVA when normal distribution (Shapiro-Wilk test) and equality of variance (Levene's test) were verified. When necessary, data were log transformed to meet ANOVA assumptions. Otherwise Kruskal-Wallis tests were performed instead. ANOVAs were followed by Tukey's honestly significant difference (HSD) post hoc tests and Kruskal–Wallis tests were followed by Mann-Whitney U-tests to separate sets of homogeneous data.

RESULTS

Photosynthetic parameters

Dark respiration (R_d) did not differ significantly among the three algal groups and averaged 0.11 µmol O_2 cm^{-2} thallus h^{-1} in terms of O_2 consumption (Table 1). The response of net photosynthesis in terms of O_2 production to irradiance (P_n-E curves) is presented in Fig 4 for each algal groups. Maximal gross photosynthesis ($P_{g\ max}$) significantly differ between algal groups (Table 1). It was minimal in clade C1 from LC and RM, averaging 0.6 µmol O_2 cm^{-2} h^{-1} and significantly higher in clade C4 from LC, reaching 0.9 µmol O_2 cm^{-2} h^{-1}. The mean ratio of $P_{g\ max}$: R_d was 6 both in clade C1 from LC and RM. It was twice higher (12) in clade C4 from LC (Table 1). The mean saturating irradiance (E_k) was the lowest in RM (25 µmol photons m^{-2} s^{-1}) and was 3- to 4-fold higher in LC algal groups. It did not differ between clades C1 and C4 from LC and averaged ca. 90 µmol photons m^{-2} s^{-1}. The compensation irradiance (E_c) followed the same pattern and was significantly lower at RM (5 µmol photons m^{-2} s^{-1}) than at LC, where it averaged 12 µmol photons m^{-2} s^{-1} (Table 1).

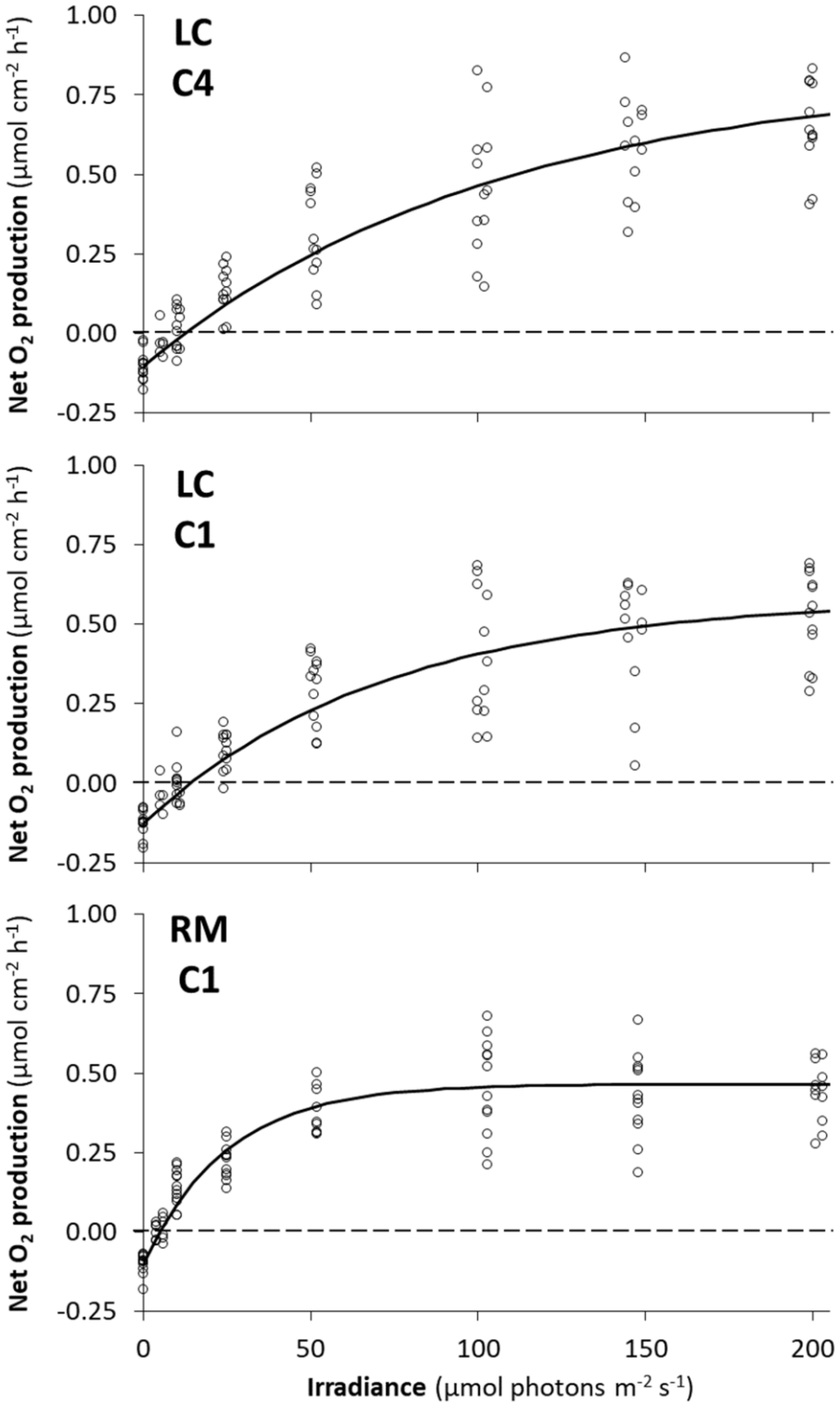

Fig. 4. Net photosynthesis versus irradiance curves in the three algal groups of the species complex *Lithophyllum stictaeforme/cabiochae*: clade C4 from LC (LC-C4), clade C1 from LC (LC-C1), and clade C1 from RM (RM-C1).

Physiological rates of photosynthesis, respiration and calcification

Dark respiration rate (R_d) was significantly lower in RM samples (0.10 ± 0.01 µmol O_2 cm^{-2} thallus h^{-1}) relative to the LC algal groups. In LC, R_d was *ca*. 50% higher, averaging 0.14 ± 0.01 µmol O_2 cm^{-2} thallus h^{-1} (Fig. 5, Table 1). Gross photosynthesis rates (P_g) were minimal in RM samples and maximal in LC samples. P_g averaged 0.5 µmol O_2 cm^{-2} h^{-1} in both RM and LC when exposed to an irradiance level of 50 µmol photons m^{-2} s^{-1} and ranged from 0.5 (RM) to 0.8 µmol O_2 cm^{-2} h^{-1} (LC) under 100 µmol photons m^{-2} s^{-1} (Figs 7, 9). No significant difference between the three algal groups was found in P_g measured at 50 or 100 µmol photons m^{-2} s^{-1} (Table 1).

Net calcification rates in the dark (G_d) significantly differed among algal groups. G_d were the lowest in the clade C4 from LC, intermediate in the clade C1 from LC, and highest in the clade C1 from RM, averaging, 0.00, 0.01, and 0.02 µmol $CaCO_3$ cm^{-2} h^{-1}, respectively (Fig. 6, Table 1). Net calcification rates in the light (G) followed the opposite trends as G_d with the lowest rates in the clade C1 from RM, intermediate in the clade C1 from LC, and the highest in the clade C4 from LC, averaging 0.11, 0.14, and 0.17 µmol $CaCO_3$ cm^{-2} h^{-1}, respectively, under 50 µmol photons m^{-2} s^{-1} and 0.13, 0.27, and 0.36 µmol $CaCO_3$ cm^{-2} h^{-1}, respectively, under 100 µmol photons m^{-2} s^{-1} (Figs 8, 10, Table 1).

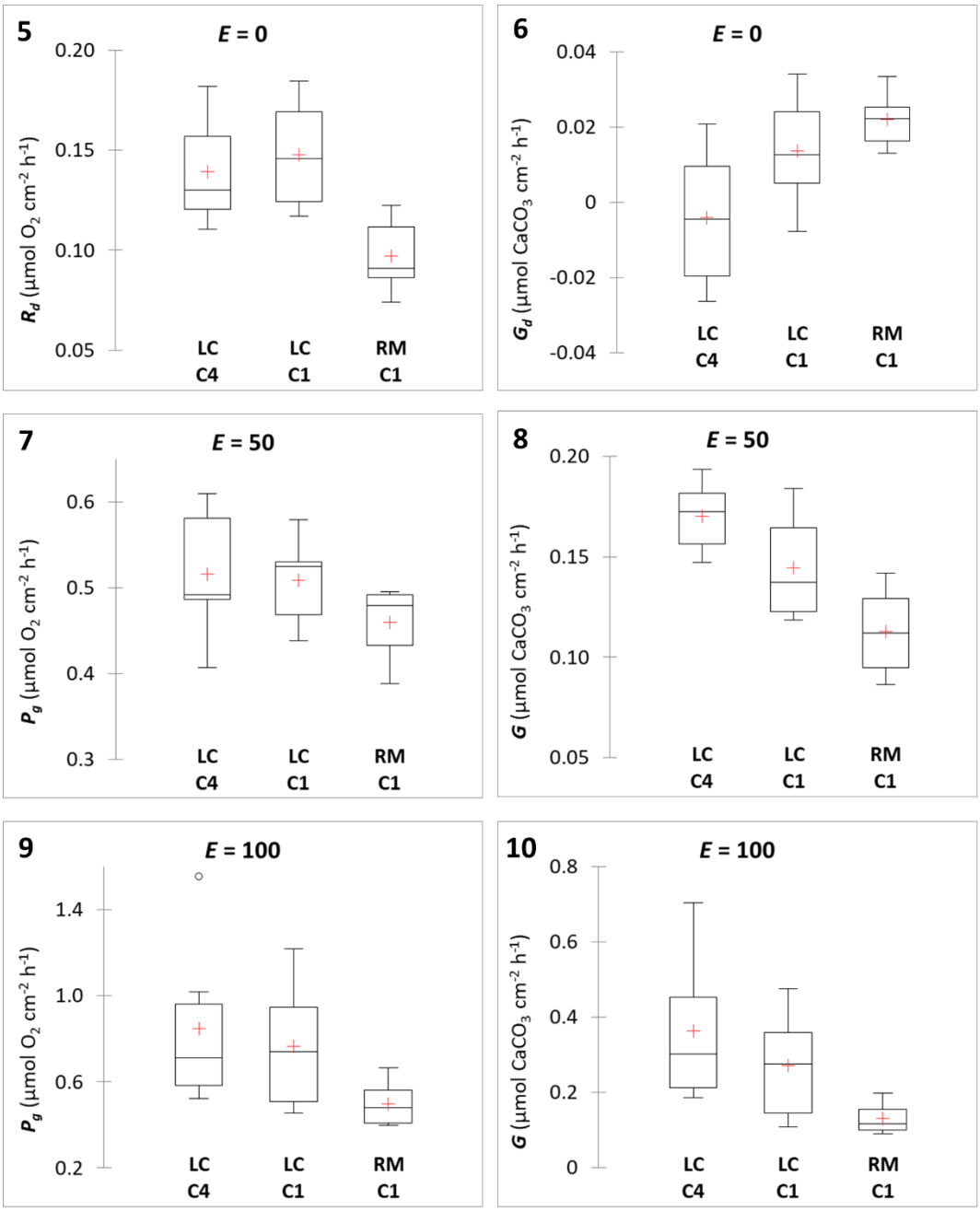

Figs 5-10. Physiological rates of respiration (R_d) and net calcification (G_d) in the dark, and gross photosynthesis (P_g) and net calcification (G) under irradiance (E) of 50 and 100 µmol photons m^{-2} s^{-1} in the three algal groups (LC-C4, LC-C1, and RM-C1) of the species complex *Lithophyllum stictaeforme/cabiochae*. Fig. 5. R_d. Fig. 6. G_d. Fig. 7. P_g under 50 µmol photons m^{-2} s^{-1}. Fig. 8. G under 50 µmol photons m^{-2} s^{-1}. Fig. 9. P_g under 100 µmol photons m^{-2} s^{-1}. Fig. 10. G under 100 µmol photons m^{-2} s^{-1}. Each box-plot has mean ("+" red cross in the box-plot), median (solid bar in the box-plot), 25th to 75th percentile (rectangular box), 1.5*interquartile range (non-outlier range of the box whiskers), and outlier values (outside box whiskers).

Diel carbon and carbonate production

At LC (28 m), diel (24-h) net organic C production (P_n) was estimated to be 4.6 and 3.5 µmol C cm^{-2} thallus d^{-1} and diel net inorganic C production (G) to 4.2 and 3.3 µmol $CaCO_3$ cm^{-2} thallus d^{-1}, in C4 and C1, respectively. At RM (45 m), diel (24-h) P_n was estimated to be 2.3 µmol C cm^{-2} thallus d^{-1} and diel G to 1.2 µmol $CaCO_3$ cm^{-2} thallus d^{-1}.

DISCUSSION

In the present study, we pointed out differences in physiological performances between the two cryptic species C1 and C4 from the same depth and light environment, and within the dominant and ubiquitous cryptic species C1 from different light-environments (different depths).

Dark respiration rates (R_d) measured in the three algal groups of the species complex *L. stictaeforme/cabiochae* (0.10-0.15 µmol O_2 cm^{-2} thallus h^{-1}) were in the range of those reported for *L. cabiochae* in similar conditions of temperature (16°C) and after exposure to darkness (Martin *et al*., 2013a). No difference was evidenced between the two cryptic species C1 and C4, from LC. However, within the C1 cryptic species, respiration rates were about 30% lower in specimens from deeper waters (RM) than those from shallower waters (LC). This result is consistent with previous studies that showed that algae living in deep habitats have low respiratory activity, a strategy to avoid excessive carbon losses (Littler *et al*., 1986; Gomez *et al*., 1997). As specimens from shallower waters present higher metabolic activities (e.g. photosynthetic and calcification rates) and are supposed to grow faster, they may require higher supply of energy produced by respiration for their growth (Zou *et al*., 2011), as evidenced here by increased respiratory activity in specimens from LC.

Photosynthetic parameters derived from photosynthesis-irradiance curves indicated that the three algal groups were typically shade-adapted macroalgae. As sublittoral species growing in deep water (28-45-m depth), *L. stictaeforme/cabiochae* is effectively acclimated/adapted to chronic low light conditions, as indicated by low values of compensation irradiance (E_c) and saturating irradiance (E_k). In the three groups of algae, the gross photosynthetic rates exceed respiratory rates at very low irradiance levels (E_c < 15 µmol photons m^{-2} s^{-1}), while low light is required to saturate photosynthesis (E_k < 100 µmol photons m^{-2} s^{-1}). E_c and E_k in *L. stictaeforme/cabiochae* were strongly related to water depth and concomitant change in light availability. E_c averaged 12 µmol photons m^{-2} s^{-1} in shallower specimens from 28-m depth, whereas an irradiance of 5 µmol photons m^{-2} s^{-1} is already sufficient for photosynthesis to exceed respiration in deeper specimens growing at 45-m depth. Similarly, E_k was only 25 µmol photons m^{-2} s^{-1} in deeper specimens, being 3.5-fold lower than in shallower specimens. We demonstrated here changes in E_k and E_c as an acclimation to ambient light, even within cryptic species (C1). Photoacclimation within species has already been observed in red soft macroalgae (Gomez *et al*., 1997; Marquardt *et al*., 2010) and CCA (Payri, 2001) from different light-environments. This ability for

photoacclimation allows the *L. stictaeforme/cabiochae* cryptic species C1 to grow in a wide range of light environments, as confirmed by its broad vertical distribution from 24 to 46 m depth and its large spatial distribution over Mediterranean coralligenous habitats (De Jode *et al*., 2019; Cinar *et al*., 2020). The C1 cryptic species is effectively the most abundant species along the French Mediterranean coastline. Its ability to acclimate to various light niches could thus contribute to its greater spatial distribution. Conversely, the cryptic species C4, which is only found in the shallowest sites along the French Mediterranean coasts (De Jode *et al*., 2019), appeared more adapted to high light. The C4 species effectively had the highest values of saturating irradiance (E_k:105 µmol photons m^{-2} s^{-1}), indicating the highest light requirements to saturate photosynthesis. Under high irradiances, the cryptic species C4 appeared particularly efficient, as evidenced by a 30% higher rate of maximum gross photosynthesis ($P_{g\ max}$) and a twice higher ratio of $P_{g\ max}/R_d$ relative to C1. Although non-significant, photosynthetic rates (P_n and P_g) were also higher in C4 than in C1 under the irradiance level of 100 photons m^{-2} s^{-1}, whereas P_n and P_g rates were similar under 50 photons m^{-2} s^{-1}. Such increased physiological rates would give the C4 cryptic species a competitive advantage in situations with higher incident irradiance, like in summer, when incident irradiances of 100 photons m^{-2} s^{-1} are reached for several hours during daytime at 28-m depth in the Bay of Marseille. Effectively, on a 24 h basis, we estimated diel net primary production to be approximately 30% higher in C4 than in C1 in shallow waters (LC). The C4 cryptic species is the second most abundant species after C1 in shallower waters in the Northern area of the Bay of Marseille (De Jode *et al*., 2019). It appears nearly restricted to zones with high irradiance, whereas species C1 (as well as less abundant species of the complex) were found also in less irradiated zones. The inability of C4 to thrive in deeper or darker zones may be due to a reduced physiological plasticity relative to C1, in agreement with its increased photosynthetic performance under higher irradiance levels relative to C1. Unfortunately, we could not investigate the physiological plasticity of C4 since it is very rare in deep habitats.

As evidenced for photosynthesis, we observed intra-and inter-cryptic species differences in the ability of *L. stictaeforme/cabiochae* to calcify. The C4 cryptic species appeared well adapted to calcify under high light but less efficient for dark calcification, whereas the C1 cryptic species has ability to calcify under both high (LC) and low (RM) light conditions, with particular shade acclimation for deeper specimens. Differences in calcification rates can be explained by species-specific differences in the ability of coralline algae to physiologically control the calcification process (Cornwall *et al*., 2017). Recent observation notably supports a species-specific control of calcification traits in Mediterranean

Lithophyllum cryptic species. Difference in cell-wall skeletal ultrastructure have been recently evidenced by Basso et al. (2022) among two morphologically similar, but genetically distinct sympatric species, *L. racemus* and *L. pseudoracemus*, even those growing in similar conditions and depth. Strong correlations between calcification and photosynthesis processes have previously been described in coralline algae (Pentecost, 1978; Borowitzka & Larkum, 1987; Chisholm, 2000; Martin *et al*. 2006, 2007, 2013a,b; Williamson *et al*., 2017) and in particular in *L. cabiochae* (Martin *et al*., 2013a,b). Photosynthesis can effectively influence calcification by providing energy and substrate (Chisholm, 2003) or favourable conditions for $CaCO_3$ precipitation by locally elevating pH at the calcification sites and in the boundary layer (Koch *et al*., 2013; Hofmann *et al*., 2016; Cornwall *et al*., 2017). Indeed, light calcification responses among *L. stictaeforme/cabiochae* algal groups follow similar patterns as those of photosynthesis. The highest calcification rates in C4 would confirm the competitive advantage of this cryptic species in high light conditions, whereas, for C1, specimens found in deeper waters (RM) had lower calcification rates relative to those from shallower waters. We evidenced here that *L. stictaeforme/cabiochae* calcification rates increased with increasing light intensity and concomitant increased photosynthetic or light-triggered processes. However, the calcification process is not totally light-dependent since calcification can occur within darkness. The continuation of calcification in the dark is supposed to rely on accumulated energy stored during periods of irradiance (McCoy & Kamenos, 2015). We previously evidenced that calcification continues to occur in the dark in *L. cabiochae* both during day-time and night-time (Martin *et al*., 2013b). Here net calcification rates in the dark were reduced but remained positive in the C1 cryptic species, while they became net negative (net $CaCO_3$ dissolution) in C4. The highest rates of dark calcification were measured in the deeper specimens from RM. They were able to maintain 20% of their calcification rates in the dark, whereas shallower specimens from LC had more than 10-fold lower dark, compared to light, calcification rates. The better performance of the deeper specimens for dark calcification confirm they have very low-light requirements for growth and are better acclimated to grow in deeper waters. Conversely, the shallower C4 cryptic species was not able to maintain positive net calcification in the dark. Increased $CaCO_3$ dissolution and/or reduced $CaCO_3$ precipitation in darkness can be related to lowered pH within cell walls or thallus surface due to respiration (McNicholl & Koch, 2021). Effectively, higher respiration rates were measured in the shallower specimens from LC and likely accounts for decreased net calcification rates.

In spite of physiological acclimation to low-light condition, specimens from deeper waters present reduced metabolic activities and lower diel (24 h) net carbon and carbonate production than those found in shallower waters. *L. stictaeforme/cabiochae* would thus grow faster at 28-m depth (LC) than at 45-m depth (RM). Associated differences in morphological traits observed between shallower and deeper specimens in C1 likely result from acclimation to depth, with reduced thallus thickness (higher surface to volume or weight ratio) in the deeper specimens. Thallus thickness in coralline algae can effectively reflect their growth strategies, *i.e*. vertical versus horizontal growth. The capacity of fast horizontal (marginal) growth of thin thalli, like those found at RM, could thus be an advantage in deep water where light is reduced (Hanelt & Figueroa, 2012).

In conclusion, our results revealed physiological plasticity within the dominant and ubiquitous *L. stictaeforme/cabiochae* cryptic species C1, that may contribute in its greater spatial distribution from shallow to deep habitats, while C4 appeared more specialized to higher levels of irradiances of shallow waters. To increase our knowledge of acclimations and differential adaptations in the cryptic *L. stictaeforme/cabiochae* species, further research should focus on physiological performances on an annual basisconsidering seasonal changes in daylength, temperature and irradiance levels. Then physiological activities under optimal conditions of temperature and irradiance in summer needs to be high enough to promote growth, reproduction, and energy storage to cope with reduced temperature and light availability during less favourable seasons (Hanelt & Figueroa, 2012). *L. stictaeforme/cabiochae* cryptic species can also differ in terms of competitive ability or resistance to environmental stresses, which could affect their distribution. Such knowledge in cryptic species-specific physiological and ecological characters are needed to anticipate their susceptibility to local and global environmental stresses (Kato *et al*., 2014). Studies on the specific cryptic species responses to environmental changes of *L. stictaeforme/cabiochae* are thus needed for a better prediction of future changes in coralligenous habitats and Mediterranean coastal ecosystems.

AKNOWLEDGMENTS

We thank Dorian Guillemain from the diving service of the Observatory of Sciences of the Universe (OSU) Pytheas Institute and Bruno Belloni, Pascal Mirleau, and Sandrine Ruitton for their help in sample collection by scuba diving. We also thank Sacha Molinari for technical help during lyophilisation and Térence Legrand for providing a map image file he has previously built. Data used in this work were partly produced through the technical facilities of the Molecular laboratory facility (SCBM) and the Experimental Aquaria facility (SCDE) of the IMBE (Marseille).

No potential conflict of interest was reported by the authors.

AUTHOR CONTRIBUTIONS

S. Martin: original concept, designed the experiment, physiological experiments, data analyses, drafting and editing manuscript; V. Calvert: set up and performed the experiment; A. Chenuil: original concept, molecular analyses, editing manuscript.

582 **REFERENCES**

583

584 Ballesteros, E. (2006). Mediterranean coralligenous assemblages: a synthesis of present
585 knowledge. *Oceanography and Marine Biology: An Annual Review*, **44**: 123-195.

586

587 Basso, D., Piazza, G. & Bracchi, V.A. (2022). Calcification traits for cryptic species
588 identification: Insights into coralline biomineralization. *PLOS One*, **17**(10): e0273505.

589

590 Borowitzka, M.A. & Larkum, A.W.D. (1987). Calcification in algae: Mechanisms and the
591 role of metabolism. *Critical Reviews in Plant Sciences*, **6**(1): 1-45.

592

593 Chenuil, A., Cahill, A. E., Délémontey, N., Du Salliant du Luc, E. & Fanton, H. (2019).
594 Problems and Questions Posed by Cryptic Species. A Framework to Guide Future Studies.
595 *From Assessing to Conserving Biodiversity. History, Philosophy and Theory of the Life*
596 *Sciences*. M. d. S. J. Casetta E., Vecchi D. (eds), Springer, Cham. 24.

597

598 Chisholm, J.R.M. (2000). Calcification by crustose coralline algae on the northern Great
599 Barrier. *Limnology and Oceanography*, **45**(7): 1476-1484.

600

601 Chisholm, J.R.M. (2003). Primary productivity of reef-building crustose coralline algae.
602 *Limnology and Oceanography*, **48**(4): 1376-1387.

603

604 Cinar, M.E., Féral, J.-P., Arvanitidis, C., David, R., Taskin, E., Sini, M., Dailianis, T., Dogan,
605 A., Gerovasileiou, V., Evcen, A., Chenuil, A., Dagli, E., Aysel, V., Issaris, Y., Bakir, K.,
606 Nalmpanti, M., Sartoretto, S., Salomidi, M., Sapouna, A., Acik, S., Dilitriadis, C.,
607 Koutsoubas, D., Katagan, T., Ozturk, B., Kocak, F., Erdogan-Dereli, D., Onen, S., Ozgen, O.,
608 Turkcu, N., Kirkim, F. & Onem, M. (2020). Coralligenous assemblages along their
609 geographical distribution: testing of concepts and implications for management. *Aquatic*
610 *Conservation: Marine and Freshwater Ecosystems*, **30**(8): 1578-1594.

611

612 Cornwall, C. E., Comeau, S. & McCulloch, M. T. (2017). Coralline algae elevate pH at the
613 site of calcification under ocean acidification. *Global Change Biology*, **23**(10): 4245-4256.

614

De Jode, A. (2018). A study of coralligenous habitats biodiversity and of the influence of environmental factors using genetic tools: from engineer species populations to communities. / Etude de la biodiversité des habitats coralligènes et de l'influence des facteurs environnementaux par des approches génétiques : des populations d'espèces ingénieures aux communautés. PhD thesis, Aix-Marseille Université, Marseille, 352 p.

De Jode, A., David, R., Haguenauer, A., Cahill, A. E., Erga, Z., Guillemain, D., Sartoretto, S., Rocher, C., Selva, M., Le Gall, L., Féral, J.-P. & Chenuil, A. (2019). From seascape ecology to population genomics and back. Spatial and ecological differentiation among cryptic species of the red algae *Lithophyllum stictiforme/L. cabiochiae*, main bioconstructors of coralligenous habitats. *Molecular Phylogenetics and Evolution*, **137**: 104-113.

Dickson, A.G., Sabine, C.L. & Christian, J.R. (Eds.) (2007). *Guide to best practices for ocean CO_2 measurements*. PICES Special Publication 3, 191 pp.

Gomez, I., Weykam, G., Kloser, H. & Wiencke, C. (1997). Photosynthetic light requirements, metabolic carbon balance and zonation of sublittoral macroalgae from King George Island (Antarctica). *Marine Ecology Progress Ser*ies, **148**: 281-293.

Haguenauer, A., Zuberer, F., Ledoux, J.B. & Aurelle, D. (2013). Adaptive abilities of the Mediterranean red coral *Corallium rubrum* in a heterogeneous and changing environment: from population to functional genetics. *Journal of Experimental Marine Biology and Ecology*, **449**: 349-357.

Hanelt, D. & Figueroa, F.L. (2012). Physiological and photomorphogenic effects of light on marine macrophytes. *Seaweed Biology. Novel Insights into Ecophysiology, Ecology and Utilization*. B. K. Wiencke C. Berlin, Heidelberg, Springer 219.

Harmelin, J.G. (2004). Environnement thermique du benthos côtier de l'île de Port-Cros (Parc national, France, Méditerranée nord-occidentale) et implications biogéographiques. *Scientific Reports of Port-Cros National Park*, **20**: 173-194.

Hofmann, L.C., Koch, M. & de Beer, D. (2016). Biotic control of surface pH and evidence of light-induced H^+ pumping and Ca^{2+}-H^+ exchange in a tropical crustose coralline alga. *PLOS One*, **11**(7): e0159057.

Hurd, C.L., Cornwall, C.E., Currie, K., Hepburn, C.D., McGraw, C.M., Hunter, K.A. & Boyd, P.W. (2011). Metabolically induced pH fluctuations by some coastal calcifiers exceed projected 22nd century ocean acidification: a mechanism for differential susceptibility? *Global Change Biology*, **17**(10): 3254-3262.

Johansen, H. W. (1981). *Coralline Algae, a First Synthesis*, CRC Press, Boca Raton, FL.

Kamiya, M. & West, J.A. (2014). Cryptic diversity in the euryhaline red alga *Caloglossa ogasawaraensis* (Delesseriaceae, Ceramiales). *Phycologia*, **53**(4): 374-382.

Kato, A., Hikami, M., Kumagai, N.H., Suzuki, A., Nojiri, Y. & Sakai, K. (2014). Negative effects of ocean acidification on two crustose coralline species using genetically homogeneous samples. *Marine Environmental Research*, **94**: 1-6.

Kirk, J. (1994). *Light and Photosynthesis in Aquatic Ecosystems* (2nd ed.). Cambridge University Press, Cambridge. 400 pp.

Koch, M., Bowes, G., Ross, C. & Zhang, X.-H. 2013. Climate change and ocean acidification effects on seagrasses and marine macroalgae. *Global Change Biology*, **19**(1): 103-132.

Littler, M.M. & Littler, D.S. (2013). The Nature of Crustose Coralline Algae and Their Interactions on Reefs. *Research and Discoveries: The Revolution of Science through Scuba*. Lang, M.A., Marinelli, R.L., Roberts, S.J. & Taylor, P.R. Smithsonian Institution Scholarly Press. 39: 199- 212.

Littler, M.M., Littler, D.S., Blair, S.M. & Norris, J.N. (1986). Deep-water plant communities from an uncharted seamount off San Salvador Island, Bahamas: distribution, abundance, and primary productivity. *Deep Sea Research*, **33**: 881-889.

679 Littler, M.M., Littler, D.S. & Dennis Hanisak, M. (1991). Deep-water rhodolith distribution,
680 productivity, and growth history at sites of formation and subsequent degradation. *Journal of*
681 *Experimental Marine Biology and Ecology*. **150**(2): 163-182.
682
683 Lüning, K. (1990). *Seaweeds. Their environment, biogeography, and ecophysiology*. Wiley
684 Interscience, London. 527 pp.
685
686 Marquardt, R., Schubert, H., Varela, D.A., Huovinen, P., Henríquez, L. & Buschmann, A.H.
687 (2010). Light acclimation strategies of three commercially important red algal species.
688 *Aquaculture*, **299**(1): 140-148.
689
690 Martin, S., Castets, M.D. & Clavier, J. (2006). Primary production, respiration and
691 calcification of the temperate free-living coralline alga *Lithothamnion corallioides*. *Aquatic*
692 *Botany*, **85**: 121-128.
693
694 Martin, S., Clavier, J., Chauvaud, L. & Thouzeau, G. (2007). Community metabolism in
695 temperate maerl beds. I. Carbon and carbonate fluxes. *Marine Ecology Progress Series*, **335**:
696 19-29.
697
698 Martin, S. & Gattuso, J.-P. (2009). Response of Mediterranean coralline algae to ocean
699 acidification and elevated temperature. *Global Change Biology*, **15**(8): 2089-2100.
700
701 Martin, S., Charnoz, A. & Gattuso, J.-P. (2013a). Photosynthesis, respiration and calcification
702 in the Mediterranean crustose coralline alga *Lithophyllum cabiochae* (Corallinales,
703 Rhodophyta). *European Journal of Phycology*, **48**(2): 163-172.
704
705 Martin, S., Cohu, S., Vignot, C., Zimmerman, G. & Gattuso, J.-P. (2013b). One-year
706 experiment on the physiological response of the Mediterranean crustose coralline alga,
707 *Lithophyllum cabiochae*, to elevated pCO_2 and temperature. *Ecology and Evolution*, **3**(3):
708 676-693.
709
710 Martin, S. & Hall-Spencer, J.M. (2017). Effects of Ocean Warming and Acidification on
711 Rhodolith/Maërl Beds. *Rhodolith/Maërl Beds: A Global Perspective*. R. Riosmena-
712 Rodríguez, W. Nelson and J. Aguirre. Cham, Springer International Publishing: 55-85.

McCoy, S.J. & Kamenos, N.A. (2015). Coralline algae (Rhodophyta) in a changing world: integrating ecological, physiological, and geochemical responses to global change. *Journal of Phycology*, **51**(1): 6-24.

McNicholl, C. & Koch, M. S. (2021). Irradiance, photosynthesis and elevated pCO2 effects on net calcification in tropical reef macroalgae. *Journal of Experimental Marine Biology and Ecology*, **535**: 151489.

Muangmai, N., Preuss, M. & Zuccarello, G. C. (2015). Comparative physiological studies on the growth of cryptic species of *Bostrychia intricata* (Rhodomelaceae, Rhodophyta) in various salinity and temperature conditions. *Phycological Research,* **63**(4): 300-306.

Payri, C. E., Maritorena, S., Bizeau, M. & Rodière, M. (2001). Photoacclimation in the tropical coralline alga *Hydrolithon onkodes* (Rhodophyta, Corallinacea) from a French Polynesian reef. *Journal of Phycology*, **37**: 223-234.

Pentecost, A. (1978). Calcification and photosynthesis in *Corallina officinalis* L. using $^{14}CO_2$ method. *British Physiological Journal*, **13**: 383-390.

Pezzolesi, L., Peña, V., Le Gall, L., Gabrielson, P. W., Kaleb, S., Hughey, J. R., Rodondi, G., Hernandez-Kantun, J. J., Falace, A., Basso, D., Cerrano, C. & Rindi, F. (2019). Mediterranean *Lithophyllum stictiforme* (Corallinales, Rhodophyta) is a genetically diverse species complex: implications for species circumscription, biogeography and conservation of coralligenous habitats. *Journal of Phycology,* **55**(2): 473-492.

Piazzi, L., Pinna, F., Ceccherelli, G. (2022). Crustose coralline algae and biodiversity enhancement: The role of *Lithophyllum stictiforme* in structuring Mediterranean coralligenous reefs. *Estuarine, Coastal and Shelf Science*, **278**: 108121

Rossi, V., Lo, M., Legrand, T., Ser-Giacomi, E., De Jode, A., Thierry De Ville D'Avray, L., Pairaud, I., Faure, V., Fraysse, M., Pinazo, C. & Chenuil, A. (2020). Small-scale connectivity of coralligenous habitats: insights from a modelling approach within a semi-opened Mediterranean bay. *Vie et Milieu / Life & Environment*, **70**(3-4): 161-174.

Sartoretto, S., Verlaque, M. & Laborel, J. (1996). Age of settlement and accumulation rate of submarine 'coralligene' (-10 to -60 m) of the northwestern Mediterranean Sea; Relation to Holocene rise in sea level. *Marine Geology*, **130**(3-4): 317-331.

Schubert, N., Hofmann, L.C., Almeida Saá, A.C., Moreira, A.C., Arenhart, R.G., Fernandes, C.P., de Beer, D., Horta, P.A. & Silva, J. (2021). Calcification in free-living coralline algae is strongly influenced by morphology: Implications for susceptibility to ocean acidification. *Scientific Reports*, **11**(1): 11232.

Steneck, R.S. (1986). The ecology of coralline algal crusts: Convergent Patterns and Adaptative Strategies. *Annual Review of Ecology, Evolution, and Systematics*, **17**: 273-303.

Thierry de Ville d'Avray, L., Ami, D., Chenuil, A., David, R. & Féral, J.P. (2019). Application of the ecosystem service concept at a small-scale: The cases of coralligenous habitats in the North-western Mediterranean Sea. *Marine Pollution Bulletin*, **138**: 160-170.

Williamson, C.J., Perkins, R., Voller, M., Yallop, M.L. & Brodie, J. (2017). The regulation of coralline algal physiology, an in situ study of *Corallina officinalis* (Corallinales, Rhodophyta). *Biogeosciences*, **14**(19): 4485-4498.

Wimart-Rousseau, C., Lajaunie-Salla, K., Marrec, P., Wagener, T., Raimbault, P., Lagadec, V., Lafont, M., Garcia, N., Diaz, F., Pinazo, C., Yohia, C., Garcia, F., Xueref-Remy, I., Blanc, P.-E., Armengaud, A. & Lefèvre, D. (2020). Temporal variability of the carbonate system and air-sea CO_2 exchanges in a Mediterranean human-impacted coastal site. *Estuarine, Coastal and Shelf Science*, **236**: 106641.

Wolf-Gladrow, D.A., Zeebe, R.E., Klaas, C., Körtzinger, A. & Dickson, A.G. (2007). Total alkalinity: The explicit conservative expression and its application to biogeochemical processes. *Marine Chemistry*, **106**(1): 287-300.

Zou, D., Gao, K. & Xia, J. (2011). Dark respiration in the light and in darkness of three marine macroalgal species grown under ambient and elevated CO_2 concentrations. *Acta Oceanologica Sinica*, **30**(1): 1-7.

Table 1

Comparison of morphological and physiological characteristics between the three algal groups (LC-C4, LC-C1, and RM-C1) of the species complex *Lithophyllum stictaeforme/cabiochae*.

		Morphological characteristics			p-values	
		LC-C4	LC-C1	RM-C1		
Surface / Volume		5.7 ± 0.4 ^{ab}	4.6 ± 0.4 ^{a}	7.0 ± 0.3 ^{b}	< **0.001**	
Surface / Weight		3.4 ± 0.3 ^{ab}	2.6 ± 0.2 ^{a}	3.9 ± 0.2 ^{b}	**0.002**	
		P_n-E curves parameters				
		LC-C4	LC-C1	RM-C1		
R_d		0.10 ± 0.01 ^{ns}	0.13 ± 0.01 ^{ns}	0.10 ± 0.01 ^{ns}	0.189	
$P_{g\ max}$		0.93 ± 0.08 ^{a}	0.71 ± 0.06 ^{b}	0.56 ± 0.04 ^{b}	**0.001**	
$P_{g\ max}$ / R_d		12 ± 3 ^{a}	6 ± 1 ^{b}	6 ± 1 ^{b}	**0.013**	
E_k		105 ± 22 ^{a}	72 ± 16 ^{a}	25 ± 2 ^{b}	< **0.001**	
E_c		12 ± 3 ^{a}	13 ± 2 ^{a}	5 ± 1 ^{b}	**0.002**	
		Physiological rates				
	E	LC-C4	LC-C1	RM-C1		
R_d	*0*	0.14 ± 0.01 ^{a}	0.15 ± 0.01 ^{a}	0.10 ± 0.01 ^{b}	**0.008**	
P_n	*50*	0.38 ± 0.04 ^{ns}	0.36 ± 0.03 ^{ns}	0.36 ± 0.02 ^{ns}	0.922	
P_g	*50*	0.52 ± 0.03 ^{ns}	0.51 ± 0.02 ^{ns}	0.46 ± 0.02 ^{ns}	0.251	
P_n	*100*	0.71 ± 0.16 ^{ns}	0.62 ± 0.12 ^{ns}	0.40 ± 0.04 ^{ns}	0.216	
P_g	*100*	0.85 ± 0.16 ^{ns}	0.77 ± 0.13 ^{ns}	0.50 ± 0.04 ^{ns}	0.133	
G_d	*0*	-0.004 ± 0.008 ^{a}	0.014 ± 0.006 ^{ab}	0.022 ± 0.003 ^{b}	**0.023**	
G	*50*	0.170 ± 0.007 ^{a}	0.145 ± 0.011 ^{ab}	0.113 ± 0.009 ^{b}	**0.002**	
G	*100*	0.364 ± 0.082 ^{a}	0.271 ± 0.059 ^{ab}	0.131 ± 0.017 ^{b}	**0.016**	¥
Diel (24-h) net carbon and carbonate production						
		LC-C4	LC-C1	RM-C1		
Diel P_n		4.6 ± 0.6^{a}	3.5 ± 0.4^{ab}	2.3 ± 0.3^{b}	**0.008**	
Diel G		4.2 ± 0.6^{a}	3.3 ± 0.4^{a}	1.2 ± 0.1^{b}	**<0.001**¥	

Results are expressed as mean ± SE (n = 12 for Morphological characteristics, P_n-E curves parameters and Diel P_n , and n =6 for Physiological rates and Diel G).

R_d and G_d are rates respiration and calcification measured in the dark (E = 0 µmol photons m^{-2} s^{-1}). P_n, P_g and G, are rates of net photosynthesis, gross photosynthesis and calcification (in µmol O_2 or $CaCO_3$ cm^{-2} thallus h^{-1}) measured in the light under 50 or 100 µmol photons m^{-2} s^{-1}. $P_{g\ max}$ is the maximum rate of gross photosynthesis (µmol O_2 cm^{-2} thallus h^{-1}), E_k (µmol photons m^{-2} s^{-1}) is the saturating irradiance and E_c is the compensation irradiance (µmol photons m^{-2} s^{-1}). Diel P_n and Diel G are 24-h net photosynthesis and calcification rates (in µmol C or $CaCO_3$ cm^{-2} thallus d^{-1}).

P-values from one-way analyses of variance (ANOVAs) (df = 2,33 for Morphological characteristics, P_n-E curves parameters and Diel P_n and df = 2,15 for Physiological rates and Diel G) are shown at right. Bold type indicates significance ($P < 0.05$). Different subscripts (a and b) indicate significant difference between algal groups ($P < 0.05$, Tukey HSD post hoc tests); ns, non-significant difference ($P > 0.05$). Transformed data are indicated: ¥ log (x). Since E_k data did not meet the assumptions of equality of variance (Levene test), differences between groups were assessed by Kruskal-Wallis ANOVA H-tests followed by Mann-Whitney U-tests to separate sets of homogeneous data.

804 **Figure legends**

805 **Fig. 1**. Map of the study area, showing the locations of the two sampling localities in the Bay
806 of Marseille: La Couronne (LC) and Riou-Moyade (RM). SOMLIT: Frioul station (*ca*. 65-m
807 depth) of the French national network of coastal observation CNRS-INSU SOMLIT (*Service*
808 *d'Observation en Milieu Littoral*).

809 **Fig. 2**. Daily mean changes in incident photosynthetically available radiation (PAR) at the
810 surface (left axis) and at 28 and 45 m depth (right axis) in July in the Bay of Marseille.

811 **Fig. 3**. Morphology of the *Lithophyllum stictaeforme*/*cabiochae* cryptic species C1 and C4
812 from "La Couronne" (LC) and "Riou-Moyade" (RM) localities. Scale = 5 cm. (Photo © S.
813 Martin).

814 **Fig. 4**. Net photosynthesis versus irradiance curves in the three algal groups of the species
815 complex *Lithophyllum stictaeforme/cabiochae*: clade C4 from LC (LC-C4), clade C1 from
816 LC (LC-C1), and clade C1 from RM (RM-C1).

817 **Figs 5-10**. Physiological rates of respiration (R_d) and net calcification (G_d) in the dark, and
818 gross photosynthesis (P_g) and net calcification (G) under irradiance (E) of 50 and 100 µmol
819 photons m^{-2} s^{-1} in the three algal groups (LC-C4, LC-C1, and RM-C1) of the species complex
820 *Lithophyllum stictaeforme/cabiochae*. Fig. 5. R_d. Fig. 6. G_d. Fig. 7. P_g under 50 µmol photons
821 m^{-2} s^{-1}. Fig. 8. G under 50 µmol photons m^{-2} s^{-1}. Fig. 9. P_g under 100 µmol photons m^{-2} s^{-1}.
822 Fig. 10. G under 100 µmol photons m^{-2} s^{-1}. Each box-plot has mean ("+" red cross in the box-
823 plot), median (solid bar in the box-plot), 25^{th} to 75^{th} percentile (rectangular box),
824 1.5*interquartile range (non-outlier range of the box whiskers), and outlier values (outside
825 box whiskers).
826
827 Scale bar: Fig.3, 5 cm.